Chapter 5

Iodine Doped Graphene for Enhanced Electrocatalytic Oxygen Reduction Reaction in PEM Fuel Cell Applications

Adriana Marinoiu, Elena Carcadea,
Mircea Raceanu and Mihai Varlam

Additional information is available at the end of the chapter

http://dx.doi.org/10.5772/intechopen.76495

Abstract

Although doped graphene based materials have been intensively investigated, as electrocatalysts for oxygen reduction reaction (ORR), there is still a number of challenges to be explored in order to design a highly active, durable, thermodynamically stable and low-cost catalyst with full recognized technological importance. The application of iodine-doped graphene in fuel cells (FC) has been recently examined as innovative nanomaterial for cathode fabrication. Up to date microscopic and spectroscopic techniques have been combined with structural and electrochemical investigations for a compendious characterization of developed ORR catalysts. The unique structure of doped graphenes is ascertained by the presence of mesopores, vacancies and high surface area, and favors the ions/electrons transportation at nanometric scale. The chapter discusses (a) how to use the existing knowledge in respect to synthesized doped graphenes and (b) how to improve the FC by taking into account these materials and have an enhanced electrochemical performance as well as long-term durability.

Keywords: fuel cell, cathode, doped graphenes, oxygen reduction reaction, iodine

1. Introduction

Due to diminishing fossil fuel resources and climate change, sustainable renewable energy sources are sought. Among the proposed clean energy sources, fuel cells are the latest developed energy conversion devices that convert the chemical energy of a fuel directly into electrical

energy. Fuel cells technology has recently evolved to address the challenges of global energy. Among them, proton exchange membrane fuel cells (PEMFC) have attracted a considerable attention as a potential power source for automotive and stationary applications due to its low temperature operation conditions, high power density and high energy conversion efficiency. Hydrogen is regarded as the most attractive fuel for PEM FC, demonstrating excellent electrochemical reactivity, highest power density, zero emissions characteristics.

The standard structure of a fuel cell consists in a solid electrolyte in contact to a porous anode and cathode on either side. A fuel cell consists of a fuel-fed anode and an oxygen-filled cathode separated by a solid polymer membrane. Diffusion layers for the reactants and product, bipolar plates to transport the reactants/product to/from the catalytic layers; end plates with current collectors and sealing gaskets are other basic components of a fuel cell. This configuration allows the transfer of ions between the two electrodes (components constituting the membrane-electrode assembly MEA). In a typical fuel cell, gaseous hydrogen reactant H_2 is continuously fed to anode side and a gaseous oxidant (air or oxygen) is fed to the cathode compartment. The electrochemical reactions occur at electrodes and the electrons will be released to the external circuit.

Appreciable progress has been made over past 20 years regarding the development of PEMFC technology. However there are still several technical challenges that need to be addressed in order to promote their commercialization.

Among the metal catalysts for the anode and cathode reactions, platinum (Pt) exhibits the largest electrocatalytic activities for the electro-oxidation of small organic compounds in the fuel from the anode and the reduction of oxygen at the cathode. In order to obtain ideal electrocatalysts for FCs with high catalytic performance and low cost, efforts have been made to develop new structured catalysts.

Recently, several technical issues for the commercialization of PEMFC including water management at the cathode, resistance reduction of the electrolyte membrane, technical realization of electrode assembly (MEA) have been addressed. Thus, in order to improve transport of water generated from electrochemical reaction at the cathode, research has been conducted on developing the mesoporous structures into the electrode [1–9]. Pt nanoparticles based on graphene support have been extensively studied due to their catalytic properties and excellent corrosion and oxidation resistance [10–12]. However, the high cost and limited resources hinder the widespread use of Pt-based catalysts and the widespread commercialization of fuel cells. To reduce the cost of FCs, numerous studies on electrocatalysts as FC electrodes were focused on manufacturing and developing alternatives to non-precious metals [13–18].

One of the major fuel cell limitations is the low rate of oxygen reduction (ORR) at the cathode, which requires a large amount of expensive Pt/C platinum catalyst. Thus, ORR plays a critical role in determining the performance of a fuel cell. ORR is a multi-electron transfer reaction with two possible main pathways: a) a direct path in one step, involving the transfer of four electrons to directly produce H_2O; b) an indirect two-step pathway, involving the transfer of two electrons for the first stage and two second electrons for the second stage to obtain water. Previous studies have shown that, with the exception of metal catalyst degradation due to

the dissolution and aggregation of metal nanoparticles, severe corrosion and oxidation of carbon materials in the actual fuel cell environment could lead to rapid loss of catalyst activity [19–21]. In this context, the unique properties of the graphene meet the basic requirements of an ideal catalyst support. Therefore, a notable effort was devoted to the design of new nanostructured catalysts dispersed on graphene support.

In the carbonaceous family, graphene is a graphite monolayer with a thickness of only 0.34 nm. It consists of carbon atoms in a sp^2 hybridization state, arranged so that each carbon atom is covalently bonded to the other three. Graphene is the two-dimensional graphite variant; is composed of a planar (two-dimensional) arrangement of carbon atoms ensconced in a hexagonal structure. Graphene possesses unique properties such as high mobility of load carriers (up to 10^5 cm^2 V^{-1} s^{-1}) superconductivity, Hall effect at room temperature, high mechanical strength (130 GPa) and high specific surface area. These properties make the material under discussion an excellent support for catalysts used in electrochemical energy systems.

Catalysts based on graphene doped with heteroatoms have proved a stable catalytic activity compared to other ORR composite electrocatalysts. As a catalytic support, compared to other carbonaceous support materials, the graphene combines the advantages of the traditional 2D graphite (high conductivity and high specific surface area) with porous structure and non-agglomerated morphology that can facilitate the deposition and dispersion of the catalyst. Moreover, the interconnected graphene network promotes the rapid transport of electrons between active sites and the electrode and increases the electroactive catalyst surface, all of which increase the catalytic activity and durability of these electrocatalysts for ORR [22–25].

The doped graphene with various heteroatoms removes the disadvantages and limitations described above by improving the catalytic performance of the electrocatalysts due to the high specific surface area and excellent conductivity. Graphene nanosheets (GNS) have exhibited large promising applications as a support for 2-D catalyst because of the following properties: first, the graphene has a large theoretical surface area of more than 2000 m^2/g), which is twice as much as that carbon nanotubes (CNTs); secondly, the graphene has a completely conjugated sp^2 hybrid structure, giving rise to very high electrical conductivity, excellent mechanical properties, and high thermal conductivity. The electronic property of the graphene is very important for its application in electrochemistry. Previous studies have shown that the mobility of electrons in the graphite suspended monolayer can reach around 2 × 105 $cm^2/(V\ s)$ at room temperature, which is higher than that of all other materials, including metals and carbon nanotubes. Doped graphene was noted to show high electrocatalytic activity for the ORR reaction.

Previous studies have found that in the case of non-Pt graphene-based nanocatalysts, there is also a charge transfer process through the graphene-metal interface, which depends on the distance and the Fermi level difference between the graphene and the supported catalysts [22].

However, metal-based electrocatalysts often suffer from some drawbacks, particularly low acidity in the acid medium specific for PEMFC environment. Doping with non-metallic heteroatom is one of the most studied nanocatalysts for the ORR reaction in PEMFC because

it has been shown that heteroatom doping can induce redistribution of graft load. In this regard, heteroatom doped graphene such as N, S, P, B have recently demonstrated that they can effectively improve the ORR catalytic activity [26–30]. It has been suggested that the dopant (whether its electronegativity toward carbon is greater (such as N, S) or lower (such as B) could create electronically loaded sites favorable for O_2 adsorption. To reduce Pt loading and the cost of electrocatalysts in fuel cells, non-Pt catalysts supported on graphene have also been developed in recent years. For N-doped graphene, the ORR catalytic activity is strongly dependent on the nitrogen types and the doping concentration. Nitrogen-doped graphene nanocomposites, have demonstrated an improved electrocatalytic activity of ORR, due to an interpenetration network formed between N and graphene, which can efficiently accelerate the reaction, the transport of ions and electrons and therefore synergistically improves the catalytic activity of ORR. The interaction between graphene support and composites may also affect the stability of electrocatalysts. For example, the strong link between N-doped sites of graphene may result in increased resistance of hybrid catalysts [25].

The main drawbacks of the mentioned catalysts are the preparation methods with multiple operating activities as well as the sophisticated equipment, making the processes less attractive to be transposed on a larger production scale. Other disadvantages are reaction conditions involving high temperatures for thermal decomposition, high vacuum or supercritical conditions.

Calculations using functional density theory (DFT) showed that the electrocatalytic activity of the heteroatom doped graphene is strongly dependent on the electronic spin density and the distribution of the electric charge density on the atoms. Catalytic active sites of doped graphene are typically high density spinning carbon atoms. N, P or B doped graphene introduces unpaired electrons and determines a local high density resulting in a high electrocatalytic ORR performance. Halogens are other important elements that offer new properties for alternative energy devices and technologies due to the effect of the difference in electronegativity between halogen atoms (x = 2.66–3.98) and C atoms (x = 2.55). They have a different electron loss capacity compared to O_2^- (x = 3.44). It is important to note that iodine halide may form partially ionized bonds to promote the transfer of the burden due to its large atomic size (the largest in the halogen group) [31–35]. In addition, it is known that the sides of the halogenated graphite have sufficient possibilities to attract O_2 and to weaken the O—O bond from the adsorbed oxygen, thus facilitating efficient conversion into water after reduction and protonation.

Previous studies have shown that the single layered basal structure of graphene can guarantee its electrochemical durability. In fact, the carbon corrosion starts from graphite defects, and carbonaceous materials with several graphite layers usually exhibit fewer structural defects. Therefore, the intrinsic grafting capacity of the graphene could improve the durability of graphene composite materials. More efforts need to be devoted to scalable and reproducible synthesis, with a compositional and morphological control, as well as investigations into properties and catalytic mechanism. In this area, major efforts have been made to refine these properties, including the adsorption of halogen molecules on the surface of the monolayer graphene as a promising approach due to the diversity of halogen properties and the variety of formed structures. The adsorption of atoms and halogen molecules on the graphene layer has been studied both theoretically and experimentally to adjust the electronic structure of the graphene layer.

Theoretically, adsorption of diatomic halogen molecules on graphene using functional Van der Waals has been studied, which includes nonlocal correlation effects, perfect for geometric optimization. The adsorption of halogen atoms on graphenes was studied using only a semi local function. It is accepted that an iodine atom can accept 0.5 electrons from the carbon substrate. The doping of the graphene through physical adsorption is particularly promising because it can increase the concentration of the carriers without affecting carrier mobility as in the case of chemical adsorbed dopants, where the covalent function can produce crystalline defects and irreversibly alter the electron structure. One of the most promising dopants that could be physically adsorbed on the graphite is iodine. Iodine is also considered to be a stable and practical dopant as compared to other halogen based dopants (Cl, Br and F) and compared to many other physically adsorbed dopants such as alkali metal dopants (K, Li, Na, etc.), acids (hydrochloric acid, HNO_3 and H_2SO_4) and organic compounds (tetracyano quinodimethane, tetrafluorotetracyanoquinodimethane), poly (4-vinylpyridine) and polyethyleneimine). However, the intercalation of iodine in the engraved Bernal multilayer graphite, which is required for potential electrode applications, was considered unlikely due to the strong interaction between the graphene layers and the high molecular size of I_2. In addition, the physicochemical properties of iodine-doped graphite, such as its chemical state, thermal stability, and working function have not been extensively investigated, even if they are critical parameters for successfully achieving graphite-based electrodes in industrial applications. It has been shown that the overlaid monolayer graphite and the double layer of graphite foil can be efficiently doped with iodine.

The request of a chemically stable material and efficient ORR electrocatalyst, directed us to develop a new concept of electrode as alternative cathode catalyst/microporous layer. The recent new application of iodine-doped (I-doped) graphene as electrode in PEMFC has been recently recognized as an improved strategy for effective modification of cathode side efficiency [32–35]. The performed experimental studies revealed that the microporous layer (MPL) placed between catalyst layer (CL) and GDL have many advantages, like: keeping the hydration of the membrane and of the ionomer phase, preventing gas diffusion layer (GDL) flooding, especially at high current densities, forming a more intimate contact between CL and GDL.

The main objective of this work is to improve the ORR performance by including of the nanostructured I-doped graphene and to prove the efficiency of the developed cathode in PEMFC operation conditions. It is important to mention, that only few papers have been reported in respect to the cathode electrocatalyst for PEMFC containing I-doped graphene. In view of these facts, the purpose of this work is to provide valuable information about the recommendation of I-doped graphene as innovative ORR electrode in the PEMFC cathode, based on performances obtained in electrochemical test in FC operation conditions.

2. Experimental

2.1. Materials

Graphite powder, $K_2S_2O_8$, P_2O_5, conc. H_2SO_4, $KMnO_4$, HI were purchased from Sigma-Aldrich., H_2O_2 and HCl were obtained from Oltchim SA Romania. Carbon paper gas diffusion layer

(GDL, SGL), membrane (Nafion-212), ionomer solution (5 wt.% Nafion) were purchased from Ion Power, USA. Commercial catalyst (HISPEC 4000 Pt/C 40 wt.%) was purchased from Alfa Aesar. The purity of reactants (H_2 and O_2) was 99.999%.

2.2. Catalysts preparation

I-doped graphene electrocatalyst was synthesized via a facile process described in detail elsewhere, through nucleophilic substitution of graphene oxide (GrO) by reduction with hydroiodic acid (HI) catalyzed by AlI_3 [24, 25]. Briefly, the graphite oxide (GO) was prepared starting from graphite powder by a modified Hummers method including specific steps, as follows. The pre-oxidation was used to prepare the preoxidized GO, namely the graphite (7.5 g), $K_2S_2O_8$ (6 g), and P_2O_5 (6 g) were introduced into conc. H_2SO_4 (50 ml) and P_2O_5 (50 g), under continuously stirring at 80°C. The product was washed, filtrated, dried at 60°C. The as pre-oxidized GO was mixed into conc. H_2SO_4, and then $KMnO_4$ (45 g) was slowly added during stirring and cooling in water-ice bath. The suspension was stirred at 40°C until it became brown, and then was diluted using de-ionized water. H_2O_2 30 wt.% (50 ml,) solution was slowly introduced. The yellow mixture was centrifuged, washed with a 1:10 HCl aqueous solution in order to remove residual metal ions. The obtained GO solution was dispersed by stirring using an IKA Ultraturrax T 25 (2 h), and ultrasonic bath (ELMA T 490DH model) at 110 W/40 kHz and 35°C (4 h). Graphene oxide (GrO) 4 g L^{-1} was obtained. Taking out a share-part of as-prepared GrO dispersion, the hydroiodic acid HI 55 wt.% (170 g) was added (in 4 h) at 80°C, as reduction agent and precursor iodine dopant. The obtained mixture was washed using de-ionized water for several times, dried to constant weight at 50°C (more than 8 h), and grated to powder. The final step was the elemental iodine removal by repeated extraction in acetone using a Soxhlet extractor.

2.3. Catalysts characterization

The microstructure and morphology of prepared samples were evaluated by using the following equipment: field emission scanning electron microscope (FESEM SU 5000 Hitachi) equipped with EDS-energy dispersive X-ray spectroscopy and WDS-wavelength dispersive; X-ray photoelectron spectroscope (XPS, Quantera SXM equipment), with a base pressure in the analysis chamber of 10^{-9} Torr and X-ray source Al K_α radiation (1486.6 eV, monochromatized) and the overall energy resolution estimated at 0.65 eV by the full width at half maximum (FWHM) of the $Au4f_{7/2}$ line; Fourier transform infrared (FTIR) spectrometer (Nicolet Impact 410, Thermo Fisher, USA); Autosorb IQ (Quantachrome, USA) with adsorption and desorption experiments performed at 77 K after initial pre-treatment of the samples by degassing at 115°C for 4 h; X-ray fluorescence spectrometer (XRF, Rigaku ZSX Primus II), equipped with an X-ray tube with Rh anode, 4.0 kW power, with front Be window of 30 μm thickness.

2.4. Electrode preparation and electrochemical measurements

2.4.1. Electrode preparation and MEA assembling

A detailed description of the electrodes and membrane electrode assembly fabrication procedure was reported in our previous studies. Summarizing, a catalyst ink was prepared by

mixing water, 5 wt.% Nafion solution (DuPont), water and isopropyl alcohol (IPA) (Aldrich), ionomer/water/isopropyl alcohol = 6/14/80 (volume), with the Pt/C catalyst (Hispec 4000 Alfa Aesar). The prepared catalyst ink was mixed in an ultrasonic bath (30°C, 2 h) and sprayed using Sono-Tek ultrasonic coating equipment (Exacta Coat, Sono-Tek Corporation, USA), at a flow rate of 0.5 ml min^{-1}, onto the both side of pretreated Nafion 212 membrane in order to fabricate the catalyst coated membrane (CCM). The catalyst loadings were 0.2 mg cm^{-2} at the anode and cathode respectively. Two procedures of operation were used: (i) ultrasonic-spray procedure of catalytic ink containing Pt/C in order to obtain 0.2 mg cm^{-2} Pt at each side and (ii) I-doped graphene 0.2 mg cm^{-2} was integrated into cathode electrode by ultrasonic-spraying on gas diffusion layer GDL (carbon paper Toray TGP-H-120). Thus, the cathode catalyst layer was modified by taking into account the deposition of I-doped graphene supplementary sprayed on GDL (EC-TP1-090T, carbon cloth Toray, USA). The as prepared electrodes were hot-pressed on GDL on each side, for 2 min at 300 kgf and 120°C. Then, the obtained membrane electrode assembly (MEA), together with silicon type gaskets were introduced in a single PEM fuel cell system with an active area of 5 cm^2 (ElectroChem, USA).

2.4.2. Electrochemical measurements

The electrochemical evaluation was performed in a single fuel cell system PEMFC with an active area of 25 cm^2 (ElectroChem, USA). The *home-made* electrochemical test station includes a configured workstation (PARSTAT 2273), fuel cell (ElectroChem, USA), DS electronic load (AMETEK Sorensen SLH 60 V/120 A 600 W), bubble-type humidifier (ARBIN DPHS 10, USA). The PEMFC was operated at 0.3 V for 0.5 h and at 0.5 V for MEA conditioning, until the stable voltage was maintained uniformly. After steady state operating conditions were maintained, the fuel cell polarization plots and ORR performances were recorded. The flow rates of reactants (100 ml min^{-1} and 250 ml min^{-1}) gases (H_2 and air) were adjusted using flow controllers (Alicat Scientific, USA) calibrated before experiments. The cell temperature and pressure were set at 60–65°C and 1 bar pressure. The relative humidity for the anode and the cathode was set to 80 and 90%, respectively. The polarization curves were taken with a scan rate of 1 mV s^{-1}. Polarization curves were taken in a galvanostatic mode with a hold time of 5 min per point. The negative and the positive sweeps were performed and the average values were presented. Cyclic voltammetry measurements were performed in a H_2/N_2 mode cell, while the N2 flow was kept to almost zero, from 1.2 to 0.05 V at a scan rate of 0.05 V/s. The developed control system based on NI c-RIO hardware was used to control the PEMFC system. The electrochemically active Pt surface area (ECSA) was derived by the integration of the inferior hydrogen adsorption peaks. The software used to control and operate the test station with the acquiring of experimental data has been developed in LabVIEW® environment.

3. Results and discussions

3.1. Morphological and structural properties of I-doped graphene

The characterization of the prepared materials was firstly performed in order to validate the structural quality and to confirm the iodine presence.

The morphology and microstructure of as-prepared samples were observed using scanning electron microscopy (SEM). I-doped graphene materials have a typical wrinkled microstructure, fluffy and almost transparent, overlapping layers, forming a cluster composed of many tiny sheets with corrugation and scrolling, building a good porosity (**Figure 1**). These features are highly valuable for PEMFC electrode applications, providing a high surface area and ensuring efficient mass transport and good catalytic sites accessibility. The energy-dispersive X-ray spectroscopy (EDX) used in addition to SEM was used as microanalysis technique for a rough appraisal of chemical composition. The EDX spectrum revealed the microanalysis of doped graphene and confirmed the iodine presence. The spectrum is dominated by peak of C, but additional elements were identified (associated **Table 1**).

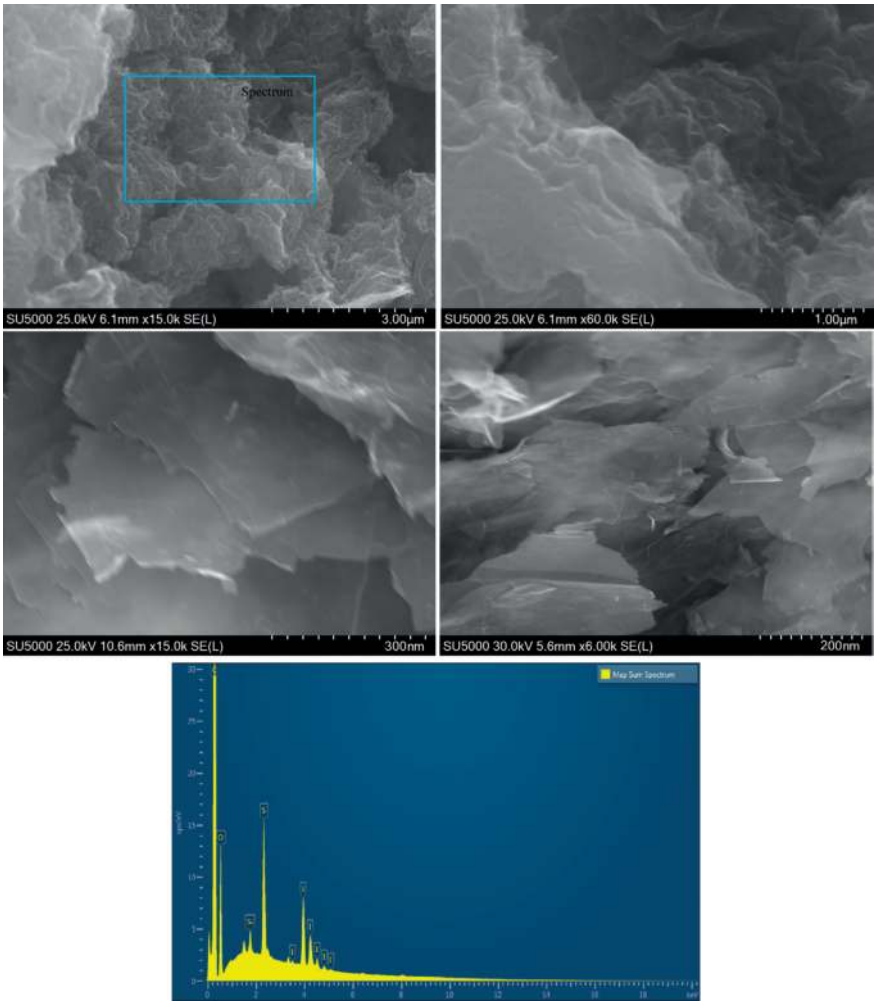

Figure 1. The SEM micrographs and EDX spectrum of prepared I-doped graphene.

http://dx.doi.org/10.5772/intechopen.76495

Element	Line type	Apparent concentration	k ratio	wt.%	wt.% sigma
C	K series	105.92	1.05920	84.39	0.15
O	K series	2.68	0.02346	13.48	0.15
Si	K series	0.30	0.00278	0.13	0.01
S	K series	2.00	0.02121	0.03	0.02
I	L series	4.06	0.05058	2.01	0.04
Total				100.00	

Table 1. Microanalysis of I-doped graphene.

The chemical composition of the I-doped graphene was investigated using X-ray photoelectron spectroscopy (XPS). Surface XPS analysis is an extremely sensitive technique (<10 nm) and was mainly focused on carbon chemistry as well as detection of iodine incorporated in the matrix at the sensitivity limit of the equipment XPS (~ 0.1% atoms). XPS spectra were collected using a monochromatic X-ray (AlK) radiation source (1486.6 eV) after the samples were placed in a 10 to 10 Torr vacuum chamber. Neutralization of the charge loading of the samples was done in dual mode using an electron gun and another argon ion. Thus, the energy calibration with the C1s line (284.8 eV) was made with great accuracy and allowed to be compared with the data from the established databases as well as from the literature [29, 30].

The introduction of chemical bonds was confirmed and high resolution spectra were collected for prominent transitions. The XPS spectra of the most prominent transitions of the chemical elements were obtained: C1s, O1s, I3d5/2, which indicated that iodine had been successfully binded on the surfaces of graphene. As anticipated, on the basis of the composition, in the survey spectra the sample show the predominant presence of carbon (1s, 284.5 eV) along with heteroatoms O (1s, 532 eV) and I (3d, 619.8 eV). High resolution C1s signals from XPS analysis are provided in **Figure 2**. High-resolution XPS spectra were further collected to quantify the doping amounts of the heteroatoms in the carbon framework. The detailed surface compositions of the prepared materials associated numerical values (chemical states rel. conc. wt.%) are systematized in **Table 2**. The C—C peak can be deconvoluted with 2

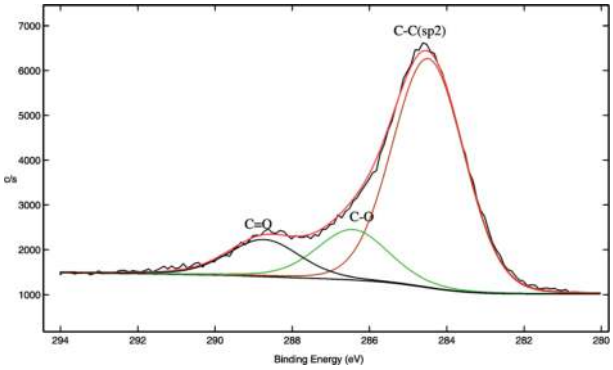

Figure 2. C1s deconvoluted spectra for C1s in I-doped graphene.

Sample	C	O	I	C—C (sp2)	C=C (sp3)	C—O	C=O	C—O=O	OH—C=O
I-doped graphene	86.1	12.4	1.5	71.0	—	16.1	—	12.9	—

Table 2. XPS data: quantification assessment, element relative concentrations (wt.%) and the chemical state relative concentrations (%).

(Gaussian-Lorentzian) curves at 284.5 eV (sp2) and 285.2 eV (sp3) binding energies (BEs). From analysis of the profile, a clear suppression of the C—O species peaks are observed, confirming the successful reduction of oxygen containing species during doping and reduction processes. Moreover, the sp^2 bonded carbon peak is sharp, suggesting an increase in the graphitic carbon configuration. I3d signal was detected as doublet 3d5/2, 3d3/2 with BEs at 619.8 eV and 624 eV.

After examination of **Table 3** it follows:

- Both the standard and ***all*** samples at studied temperatures (60 and 80°C) and different times (4, 8, 24, 28 and 48 h) show *iodine* in their matrix.
- The amount of iodine is at the XPS detection limit (~ 0.1 atom%, ~ 1 wt.%) but still can be detected and quantified
- The samples treated at temperature of 60°C show a higher iodine concentration (~ 0.15 atom%, ~ 1.5 wt.%) than those treated at 80°C (~ 0.11 atom%, ~ 1.15 wt.%).
- Both samples at 28 h (both 60 and 80°C) show a particularity: the 60°C sample shows a diffusion tendency of iodine from the surface in volume, while sample 80°C segregates iodine from the volume to the surface.
- Samples 48 h (both 60 and 80°C) show the highest relative oxygen concentration accompanied by the lowest C concentration. This phenomenon is due to oxygen segregation in volume at the surface of the samples.

The doping of iodine heteroatom into graphene is expected to produce some changes in surface area and pore size of prepared material. Due to the porous appearance of the materials confirmed by SEM analysis and of the need to obtain a high surface area for efficient ORR performance, we subsequently analyzed the surface area. In order to investigate the structure and to characterize the porosity of prepared iodine doped graphene, the nitrogen adsorption–desorption isotherms were studied using Brunauer-Emmett-Teller (BET) and are provided in **Figure 3**. The surface area was determined to be 480 $m^2\ g^{-1}$. The hysteresis study also revealed that hysteresis loops showed parallel adsorption and desorption branches. Such behavior was regarded as Type H1 among the IUPAC classification. This observation allows a better understanding of the porous features of the prepared samples, in the sense to be open at end, but unconnected to each other. As shown, the isotherm curves of adsorption/desorption performance of samples were compatible with isotherm Type IV, with an abrupt increase at high relative pressure, with respect to IUPAC classification. Based on the mentioned classification, a mainly mesoporous structure was estimated for the electrocatalyst samples.

http://dx.doi.org/10.5772/intechopen.76495

Sample/treatment conditions	Chemical element		
	C1s	O1s	I3d5/2
I-doped graphene fresh material	90.04/86.02	9.81/12.48	0.15/1.50
I-doped grapheme/T = 60°C; t = 8 h	91.56/87.89	8.29/11.69	0.15/1.52
I-doped graphene/T = 60°C; t = 24 h	91.35/87.62	8.50/10.86	0.15/1.52
I-doped graphene/T = 60°C; t = 4 h	90.69/86.87	9.17/11.69	0.14/1.44
I-doped graphene/T = 60°C; t = 28 h	91.44/88.01	8.44/10.82	0.12/1.17
I-doped graphene/T = 60°C; t = 48 h	87.59/83.13	12.27/15.51	0.14/1.36
I-doped graphene/T = 80°C; t = 4 h	90.74/87.10	9.14/11.69	0.12/1.21
I-doped graphene/T = 80°C; t = 8 h	88.22/84.04	11.67/14.81	0.11/1.16
I-doped graphene/T = 80°C; t = 24 h	88.05/83.90	11.85/15.04	0.11/1.06
I-doped graphene/T = 80°C; t = 28 h	90.05/86.14	9.82/12.51	0.13/1.34
I-doped graphene/T = 80°C; t = 48 h	81.28/75.79	18.60/23.11	0.11/1.10

Table 3. XPS experimental data for chemical stability: the studied samples and the atomic concentrations (%) and mass (mass%) at all samples, all temperatures and time intervals.

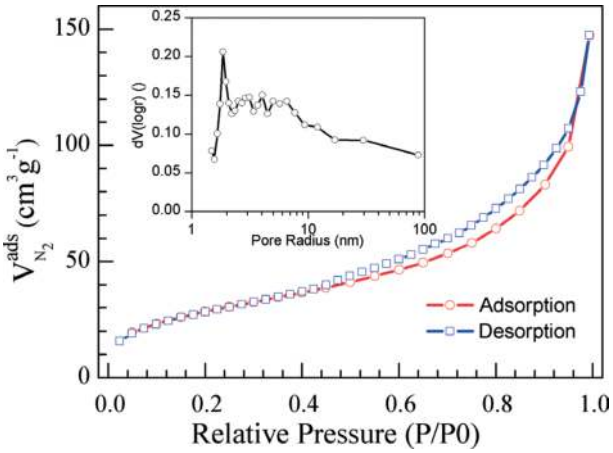

Figure 3. BET isotherm corresponding to I-doped graphene.

Barrett-Joyner-Halenda (BJH) method was utilized to measure the porous texture of prepared iodine doped graphene. A few ultramicropores in the doped graphene material are present, based on the fact that I-doped graphene possess a vertical uptake under $P/P_0 = 0.04$. A hysteresis loop type H1, from $P/P_0 = 0.4$ to $P/P_0 = 1.0$ due to the co-existence of both micropores, mesopores and some macroporous could be observed, the latter possessing a slit-like structure and most likely attributed to the pores between individual graphene sheets. This observation suggests there are good transport properties among the microspores, mesoporous and macroporous channels in I-doped graphene.

A briefly analysis on pore size distribution provided by the desorption branch using the BJH calculation approach was carried out. The pore size distribution curves presented in inserted plot, estimated according to BJH method, confirm that the greater part of the pores in the synthesized materials have size below 4.5 nm. The related curve of pore sizes highlighted a specific mesoporous structure, composed by primary and secondary pores. It is well known that the pores in an ORR catalyst layers must act two complementary roles, namely the primary pores, up to 0.04 μm, work as reaction volume, while secondary pores, from 0.04 to 0.1 μm, play the gas channel role in the porous structure [36]. As pore size distribution for I-doped graphene appears, although the samples possess limited primary structure, a structure of secondary pores is well confirmed, indicating that the transport properties in catalyst volume could be successfully obtained also after doping process.

3.2. Electrochemical characterization of I-doped graphene

Based on the structural information presented above, the prepared iodine doped graphene was evaluated as ORR cathode under practical FC operation conditions. It is easy to anticipate a better performance of cathode including the catalytic system Pt/C and I-doped graphene, mainly based on our recently results [34–36], in comparison to commercial Pt/C. This improvement in performance is likely due to higher electrical conductivity and the durability parameters, essential for the PEMFC commercialization. The fuel cell performance was characterized by measuring current-voltage polarization curves under various experimental conditions.

The testing cell is based on a 5 cm^2 single cell system using 0.2 mg Pt cm^{-2} loading as anode catalyst and the developed cathode (0.2 mg Pt cm^{-2} loading sprayed on the membrane and 0.2 mg I-doped graphene cm^{-2} loading sprayed on the GDL acting the MPL role).

The sensitivity of the fuel cell performance to the cathode side microstructure is analyzed by experimental investigations and numerical simulations, the results being reported in **Figure 4**.

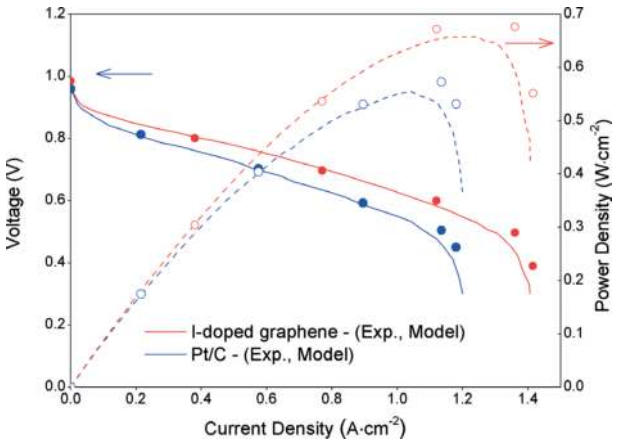

Figure 4. Polarization curves/power density plots (line) and model results (dots) for the PEMFC with cathode: commercial Pt/C (blue), and I-doped graphene (red). Cell runs with H_2/air, 1 bar anode and cathode back pressure; temperature 65C; flow rates H_2/air: 100 ml min^{-1}/250 ml min^{-1}.

One fuel cell with standard cathode configuration based on a commercial Pt catalyst and one fuel cell with an I-doped graphene layer placed between cathode GDL and CL have been considered.

The experimental data are represented as polarization and power density curves, while the numerical simulations are given as points on the curves. The numerical results for the cases investigated are in good agreement with experimental data, imparting the confidence that the computational fluid dynamics (CFD) models can be used as design tool for future improvements, and also to analyze how the fuel cell performs locally. Insightful information on the distribution and uniformity of phenomena that are taking place inside a fuel cell can be obtained by CFD modeling.

In general, the CFD simulation of FC is based on the following phases: development of the geometry; meshing the geometry (splitting into finite volumes) to obtain the computational grid; setting the mathematical model for domains and boundaries (domains for solid and gas-liquid phases, inlet and outlet gas supply system and gas channels, walls, layers combinations and electrode contacts); setting the boundary conditions; running the case for calculating parameters of interest; visualization of calculated results.

In order to compare the performances of the developed cathode versus commercial Pt catalyst with same loading, each FC performance reflected in its polarization curve was carried out. Analyzing the results, it can be seen that I-doped graphene coated GDL can lead to significant improvement in the performance of the fuel cell, up to an average of 20% in terms of both current and power density. The high electrical conductivity of the I-doped graphene layer enhanced the electrical contact between the GDL and CL, leading to an improved performance for all regions of the polarization curve. The microstructure optimization of this microporous layer based on I-doped graphene (high specific surface area, excellent mechanical properties, high thermal and electrical conductivity) promotes the rapid transport of electrons between active sites and the electrode and increases the electroactive catalyst surface, hence the increase of the performance.

3.3. CFD models developed to investigate the PEMFC performance

In addition to the global performance curves, it is important to analyze how the fuel cell performs locally. Namely, the profiles of the key variables within the components of the fuel cell could give information on the uniformity of distributions for these variables. Less uniform distribution of some key variables, e.g., the current density, can lead to the presence of some undesirable phenomena such as hotspots or flooding, thus negatively affecting the lifetime and durability of the fuel cell. In direct connection with the uniformity of key variables it is the microstructure of the fuel cell layers. This complex microstructure (gas pores, carbon particles, Pt catalyst particles, ionomer network) and the possible interactions between fluids (H_2, O_2 and all water phases) are taken into consideration in our study by CFD models developed to investigate the PEM fuel cells performance. The mass transport resistance due to the catalyst microstructure (resistance due to an ionomer film or due to a liquid water film surrounding particles), the liquid water transport through hydrophobic porous layers and the two-phase flow (liquid saturation) in the gas channels are taken into account in our model developed *based on ANSYS Multiphysics software and PEM fuel cell Module.*

Figure 5 shows the distribution of the current density for 0.5 V potential differences between anode and cathode external walls. The plane displayed is at the interface between the cathode catalyst layer and the MPL for both cases investigated. The cathode having I-doped graphene and Pt/C exhibited 85 m^2 Pt g^{-1}, which is about 2.5 times higher than that of commercial Pt/C electrode at the same Pt loading (38 m^2 Pt g^{-1}). These values were taken into consideration in the simulations and the results show clearly the increase of current density value for the FC with higher active area. An average current density of 1.135 A/cm^2 (**Figure 5** left) was obtained for the commercial Pt/C electrode, compared to 1.36 A/cm^2 for the I-doped graphene case (**Figure 5** right). The current density profile is directly linked to the distribution of the water mass fraction at the interface between the cathode catalyst layer and the adjacent MPL, as can be seen in **Figure 6**. A proper water management and a uniform distribution within the fuel cell assist in humidifying the membrane and increasing the performance. It can be concluded that the higher mesoporous and macro porous nanostructures of the I-doped graphene coated

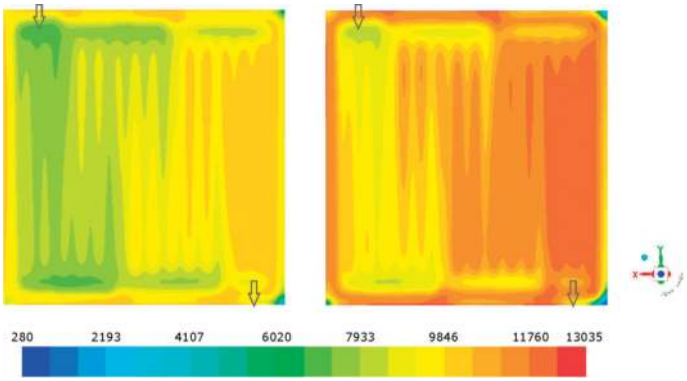

Figure 5. Current density profile for 0.5 V at the interface between the cathode catalyst layer and the MPL for the PEMFC with: commercial Pt/C (left), and I-doped graphene (right).

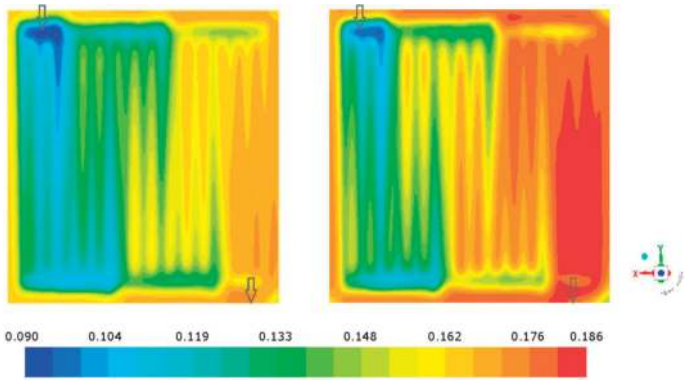

Figure 6. Water mass fraction profile for 0.5 V at the interface between the cathode catalyst layer and the MPL for the PEMFC with: commercial Pt/C (left), and I-doped graphene (right).

http://dx.doi.org/10.5772/intechopen.76495

GDL facilitate the mass transport of oxygen into the catalyst layer, the removal of water molecules from the electrolyte, ensure a conductive paths for the ions and electrons during the global transport process, resulting in a better performance in ohmic and mass transport regions of the polarization curves.

In order to examine the electrochemical stability of I-doped graphene cathode in comparison with Pt/C cathode, the electrodes were tested in the *in-situ* experiment by cyclic voltammetry (CV) measurements, elaborated in Experimental Section. The cyclic voltammetry results are presented in **Figure 7**. The CV curves show three characteristic potential regions: the hydrogen adsorption/desorption region (0.05–0.4 V), double layer plateau region and the formation and reduction of surface Pt oxide. All curves present a well-defined hydrogen adsorption/desorption region.

Operating conditions used are from experiments.

The electrochemical active area of the electrocatalysts were evaluated from the integrated area under the adsorption peaks from CV, representing the total charge associated with H^+ adsorption on metal. Thus, the cathode having Pt/C + I-doped graphene exhibited 85 m^2 Pt g^{-1}, which is about 2.5 times higher than that of commercial Pt/C electrode at the same Pt loading (38 m^2 Pt g^{-1}). This higher active area suggests more platinum sites available for the ORR which leads to the improved FC performances seen in the polarization curves. Generally, the utilization of Pt dispersed on the catalyst support is proportional to the surface area of Pt nanoparticles in contact with the electrolyte, so the ECSA results indicate that interface between catalyst and ionomer increases as effect of I-graphene added into the catalyst layer [29, 33].

Moreover, the open pores and vacancies could serve as active intercalation sites, contributing to the high charge transfer based on the conductive nanosheets with large surface area and a continuous electronic pathway, providing a high electrode-electrolyte contact interface. The mentioned synergistic effects could not only improve the ions and electrons transportation with nanometer-scale diffusion but also limits the ohmic resistance losses with big contribution to electrode stability in PEMFC device.

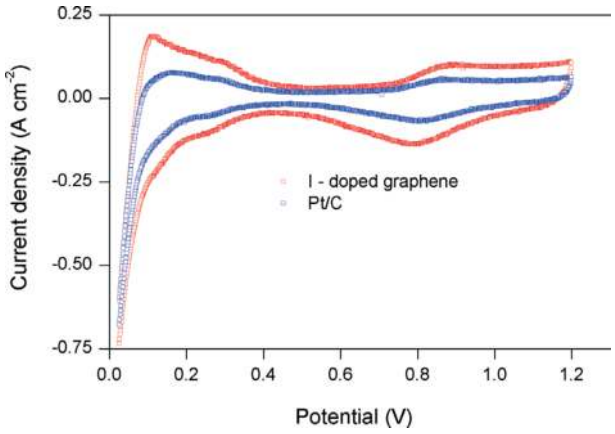

Figure 7. Cyclic voltammetry performed on *in situ* FC measurements in following operation conditions: temperature—60°C; the air in the original FC cathode was replaced with N_2; potential scan rate—50 mV/s.

4. Conclusions

In order to improve the activity and stability of PEMFC catalysts it is necessary to explore more stable catalyst for ORR. Iodine doped graphene was prepared and tested as ORR catalyst. The preparation is seen as overall process as facile, does not require complicated steps and is appropriate for scaling up. The surface compositions of I-doped graphene were analyzed by XPS. The XPS spectra of the most prominent transitions of the chemical elements were obtained: C1s, O1s, I3d 5/2, which indicated that iodine had been successfully binded on the surfaces of graphene. The chemical stability of I-doped graphene was tested in order to assess long-term performance. Insightful information on the distribution and uniformity of phenomena that are taking place inside a fuel cell are obtained from the CFD model used to analyze how this electrochemical device performs locally. The numerical results for two cases investigated (Pt/C with ECSA 35 m^2/g and I-doped graphene with ECSA 85 m^2/g) are validated by experimental data and a good agreement between modeling and experimental data were found. An overall 20% increase in current density was obtained while increasing the electrochemically active surface area (ECSA). The experimental results provide a simple route to synthesize I-doped graphene with potential application for advanced energy storage, as well as useful information to design new graphene base materials. In conclusion, we have designed a novel hybrid structure with enhanced electrochemical performances. The power output can be attributed to synergistic effects from graphene and iodine providing high utilization of Pt and better mass transport in the catalyst layer.

Acknowledgements

This work is supported by the Ministry of Research and Innovation from Romania by the National Plan of R & D, Project PN 18 12 01 02 and PN 18 12 01 04. The authors thank to Dr. Fiz. Catalin Ducu for SEM analysis and to Math. Catalin Capris for experimental study.

Conflict of interest

The authors declare that there is no conflict of interest.

Author details

Adriana Marinoiu[1]*, Elena Carcadea[1], Mircea Raceanu[1,2] and Mihai Varlam[1]

*Address all correspondence to: adriana.marinoiu@icsi.ro

1 RD Institute for Cryogenics and Isotopic Technologies—ICSI, Rm Valcea, Romania

2 University Politehnica of Bucharest, Bucharest, Romania

References

[1] Gasteiger HA, Marković NM. Just a dream—Or future reality? Science. 2009;**324**(5923): 48-49. DOI: 10.1126/science.1172083

[2] Sang MK, Chi-Yeong A, Yong-Hun C, Sungjun K, Wonchan H, Segeun J, Sungsoo S, Gunhee L, Yung-Eun S, Mansoo C. High-performance fuel cell with stretched catalyst-coated membrane: One-step formation of cracked electrode. Scientific Reports. 2016;**6**:26503. DOI: 10.1038/srep26503

[3] Barbir F. PEM Fuel Cells. In: Sammes N, editor. Fuel Cell Technology. Engineering Materials and Processes. London: Springer; DOI: 10.1007/1-84628-207-1_2

[4] Namgee J, Sang MK, Do HK, Dong YC, Yun SK, Young-Hoon C, Yong WC, Changhyun P, Kahp-Yang S, Yung-Eun S. High-performance hybrid catalyst with selectively functionalized carbon by temperature-directed switchable polymer. Chemistry of Materials. 2013;**25**(9):1526-1532. DOI: 10.1021/cm303691e

[5] Sinha PK, Mukherjee PP, Wang CY. Impact of GDL structure and wettability on water management in polymer electrolyte fuel cells. Journal of Materials Chemistry. 2007;**17**:3089-3103. DOI: 10.1039/B703485G

[6] Li H, Tang Y, Wang Z, Shi Z, Wu S, Song D, Zhang J, Fatih K, Zhang J, Wang J, Liu Z, Rami A, Mazza A. A review of water flooding issues in the proton exchange membrane fuel cell. Journal of Power Sources. 2008;**178**(1):103-117. DOI: 10.1016/j.jpowsour.2007.12.068

[7] Tanuma T. Ex situ characterization method for flooding in gas diffusion layers and membrane electrode assemblies with a hydrophilic gas diffusion layer. Journal of Fuel Cell Science and Technology. 2015;**12**(6):061002. DOI: 10.1115/1.4031917

[8] Slade S, Campbell S, Ralph T, Walsh F. Ionic conductivity of an extruded Nafion 1100 EW series of membranes. Journal of the Electrochemical Society. 2002;**149**(12):1556-1564. DOI: 10.1149/1.1517281

[9] Cho H, Kim SM, Kang YS, Kim J, Jang S, Kim M, Park H, Bang JW, Seo S, Suh KY, Sung YE, Choi M. Multiplex lithography for multilevel multiscale architectures and its application to polymer electrolyte membrane fuel cell. Nature Communications. 2015;**6**:8484. DOI: 10.1038/ncomms9484

[10] Kim OH, Cho YH, Kang SH, Park HY, Kim M, Lim JW, Chung DY, Jae Lee MJ, Choe H, Sung YS. Ordered macroporous platinum electrode and enhanced mass transfer in fuel cells using inverse opal structure. Nature Communications. 2013;**4**:2473. DOI: 10.1038/ncomms3473

[11] Hubert AG, Shyam SK, Bhaskar S, Frederick TW. Activity benchmarks and requirements for Pt, Pt-alloy, and non-Pt oxygen reduction catalysts for PEMFCs. Applied Catalysis B: Environmental. 2005;**56**(1-2):9-35. DOI: 10.1016/j.apcatb.2004.06.021

[12] Jiang L, Fan Z. Design of advanced porous graphene materials: From graphene nanomesh to 3D architectures. Nanoscale. 2014;**6**:1922-1945. DOI: 10.1039/C3NR04555B

[13] Liu J, Takeshi D, Sasaki K, Stephen M. Defective graphene foam: A platinum catalyst support for PEMFCs. Journal of the Electrochemical Society. 2014;**161**(9):838-844. DOI: 10.1149/2.0231409jes

[14] Zhu C, Dong S. Recent progress in graphene-based nanomaterials as advanced electrocatalysts towards oxygen reduction reaction. Nanoscale. 2013;**5**:1753-1767. DOI: 10.1039/C2NR33839D

[15] Shao Y, Zhang S, Wang C, Nie Z, Liu J, Wang Y, Lin Y. Highly durable graphene nanoplatelets supported Pt nanocatalysts for oxygen reduction. Journal of Power Sources. 2010;**195**(15):4600-4605. DOI: 10.1016/j.jpowsour.2010.02.044

[16] Reshetenko TV, Kim HT, Kweon HJ. Cathode structure optimization for air-breathing by application of pore-forming agents. Journal of Power Sources. 2007;**171**(2):433-440. DOI: 10.1016/j.jpowsour.2007.05.105

[17] Wang DW, Su D. Heterogeneous nanocarbon materials for oxygen reduction reaction. Energy & Environmental Science. 2014;**7**:576-591. DOI: 10.1039/C3EE43463J

[18] Bing Y, Liu H, Zhang L, Ghosh D, Zhang J. Nanostructured Pt-alloy electrocatalysts for PEM fuel cell oxygen reduction reaction. Chemical Society Reviews. 2010;**39**:2184-2202. DOI: 10.1039/B912552C

[19] Cho YH, Jung N, Kang YS, Chung DY, Lim JW, Choe H, Cho YH, Sung YE. Improved mass transfer using a pore former in cathode catalyst layer in the direct methanol fuel cell. International Journal of Hydrogen Energy. 2012;**37**(16):11969-11974. DOI: 10.1016/j.ijhydene.2012.05.031

[20] Zhao J, He X, Wang L, Tian J, Wan C, Jiang C. Addition of NH_4HCO_3 as pore-former in membrane electrode assembly for PEMFC. International Journal of Hydrogen Energy. 2007;**32**(3):380-384. DOI: 10.1016/j.ijhydene.2006.06.057

[21] Liang J, Du X, Gibson C, Qiao W. N-doped graphene natively grown on hierarchical ordered porous carbon for enhanced oxygen reduction. Advanced Materials. 2013;**25**(43):6226-6231. DOI: 10.1002/adma.201302569

[22] Minmin L, Ruizhong Z, Wei C. Graphene-supported nanoelectrocatalysts for fuel cells: Synthesis, properties, and applications. Chemical Reviews. 2014;**114**(10):5117-5160. DOI: 10.1021/cr400523y

[23] Huimin W, David W, Huakun L. Durability investigation of graphene-supported Pt nanocatalysts for PEM fuel cells. Journal of Solid State Electrochemistry. 2011;**15**(5):1057-1062. DOI: 10.1007/s10008-011-1317-8

[24] Krishna R et al. Facile synthesis of hydrogenated reduced graphene oxide via hydrogen spillover mechanism. Journal of Materials Chemistry. 2012;**22**:10457-10459. DOI: 10.1039/C2JM30945A

[25] Li M, Zhang L, Xu Q, Niu J, Xia Z. N-doped graphene as catalysts for oxygen reduction and oxygen evolution reactions: Theoretical considerations. Journal of Catalysis. 2014;**314**:66-72. DOI: 10.1016/j.jcat.2014.03.011

[26] Shuo D. Molecular doping of graphene as metal-free electrocatalyst for oxygen reduction reaction. Chemical Communications. 2014;**50**:10672-10675

[27] Stefano A, Marco F. Doping graphene with boron: A review of synthesis methods, physicochemical characterization, and emerging applications. Journal of Materials Chemistry A. 2016;**4**:5002-5025. DOI: 10.1039/C5TA10599D

[28] Marinoiu A, Teodorescu C, Carcadea E, Raceanu M, Varlam M, Cobzaru C, Stefanescu I. Graphene-based materials used as the catalyst support for PEMFC applications. Materials Today: Proceedings. 2015;**2**(6):3797-3805. DOI: 10.1016/j.matpr.2015.08.013

[29] Marinoiu A, Raceanu M, Carcadea E, Varlam M, Stefanescu I. Iodinated carbon materials for oxygen reduction reaction in proton exchange membrane fuel cell. Scalable synthesis and electrochemical performances. Arabian Journal of Chemistry. DOI: 10.1016/j.arabjc.2016.12.002 (in press)

[30] Marinoiu A, Raceanu M, Carcadea E, Varlam M, Stefanescu I. Low cost iodine intercalated graphene for fuel cells electrodes. Applied Surface Science. 2017;**424**:93-100. DOI: 10.1016/j.apsusc.2017.01.295

[31] Marinoiu A, Raceanu M, Carcadea E, Varlam M, Stefanescu I. Doped graphene as nonmetallic catalyst for fuel cells. Materials Science. 2017;**23**:108-113. DOI: 10.5755/j01.ms.23.2.16216

[32] Damien T, Pascal P, Iann CG. Theoretical study of graphene doping mechanism by iodine molecules. Journal of Physical Chemistry C. 2015;**119**(21):12071-12078. DOI: 10.1021/acs.jpcc.5b03246

[33] Marinoiu A, Raceanu M, Carcadea E, Varlam M, Stefanescu I, Enachescu M. Iodine-doped graphene for enhanced electrocatalytic oxygen reduction reaction in proton exchange membrane fuel cell applications. Journal of Electrochemical Energy Conversion and Storage. 2017;**14**:31001. DOI: 10.1115/1.4036684

[34] Marinoiu A, Teodorescu C, Carcadea E, Raceanu M, Varlam M, Cobzaru C, Stefanescu I. Convenient graphene based materials as potential candidates for low cost fuel cell catalysts. Reaction Kinetics, Mechanisms and Catalysis. 2016;**118**:281-296. DOI: 10.1007/s11144-016-1016-7

[35] Marinoiu A, Teodorescu C, Carcadea E, Raceanu M, Varlam M, Cobzaru C, Stefanescu I. An experimental approach for finding low cost alternative support material in PEM fuel cells. Revue Roumaine de Chimie. 2016;**61**(4-5):433-440

[36] Lale IS, Vildan B, Ghobad S. Engineered catalyst layer design with graphene-carbon black hybrid supports for enhanced platinum utilization in PEM fuel cell. International Journal of Hydrogen Energy. 2017;**42**(2):1085-1092. DOI: 10.1016/j.ijhydene.2016.08.210